

Berry phase induced entanglement of hole-spin qubits in a microwave cavity

Marcin M. Wysocki^{*}, Marcin Płodzień[✉], and Mircea Trif[†]

International Research Centre MagTop, Institute of Physics, Polish Academy of Sciences, Aleja Lotników 32/46, PL-02668 Warsaw, Poland



(Received 28 January 2021; revised 17 May 2021; accepted 28 June 2021; published 8 July 2021)

Hole spins localized in semiconductor structures, such as quantum dots or defects, serve in the realization of efficient gate-tunable solid-state quantum bits. Here, we study two electrically driven spin-3/2 holes coupled to the electromagnetic field of a microwave cavity. We show that the interplay between the non-Abelian Berry phases generated by local time-dependent electrical fields and the shared cavity photons allows for fast manipulation, detection, and long-range entanglement of the hole-spin qubits in the absence of any external magnetic field. Owing to its geometrical structure, such a scheme is more robust against external noises than conventional hole-spin qubit implementations. These results suggest that hole spins are favorable qubits for scalable quantum computing by purely electrical means.

DOI: [10.1103/PhysRevB.104.L041402](https://doi.org/10.1103/PhysRevB.104.L041402)

Introduction. Spin-based solid-state quantum bits (qubits) are among the most desirable platforms for implementing a quantum processor as they are inherently scalable, they interact weakly with the environments, and can be integrated efficiently with electronics [1–11].

Electric fields, instead of the conventional magnetic fields, are preferred for quantum manipulation as they can be applied locally, can be made strong, and can be switched on and off fast. Spins in solids, and specifically in semiconductors, can experience strong spin-orbit interactions (SOIs) that allow for coherent electrical spin control. Most of the implementations and proposals rely on the SOI mechanism facilitated by the presence of a static magnetic field that breaks the time-reversal symmetry. However, generating such a coupling purely electrically, without breaking this symmetry, would be advantageous as it would deactivate various dephasing mechanisms that rely on charge fluctuations, such as phonons and gate voltage noise [12–16].

A variety of schemes that utilize the *non-Abelian* geometric phase acquired by the spin qubit states in the presence of SOI and external electrical fields have been proposed for manipulating geometrically spins in solid-state devices without the need for an applied magnetic field [17–20]. Of particular interest are the hole-spin qubits realized in the $S = 3/2$ valence band of many semiconductors [17,20]. They possess strong SOI, and the p -type character of the orbital wave functions leads to a suppression of the hyperfine coupling to the surrounding nuclei [21]. Experimentally, hole spins have been under intense scrutiny recently [15,16,21–26], and a lot of progress has been made implementing conventional one- and two-qubit gates [25–30]. Building on the original works by Avron *et al.* [31,32], in Refs. [17,20] it has been shown explicitly how single *geometrical* hole-spin qubit gates [33] can be implemented using only electrical fields. However,

to the best of our knowledge, leveraging the geometry of the hole-spin states in order to implement two-qubit gates and create entanglement has yet to be demonstrated. Such geometrical entanglement is potentially more robust since it is not affected by gate timing errors and various control voltage inaccuracies. In this Letter, we make this step and propose a way to create entanglement between hole-spin qubits utilizing their non-Abelian geometric structure, local electric fields, and the photons in a microwave cavity. We show that (i) the cavity photons become imprinted with the Berry phases generated during the single hole-spin qubit gates, allowing for an efficient nondestructive qubit readout, and (ii) the interplay between photons and the non-Abelian geometry of the states allows for long-range, entangling hole-spin qubit interactions of a geometrical origin. Moreover, such a coupling is only present when both qubits are electrically driven, making it ideal for selectively coupling hole spins.

System and model Hamiltonian. We consider the system shown in Fig. 1, which consists of two *electrically* driven

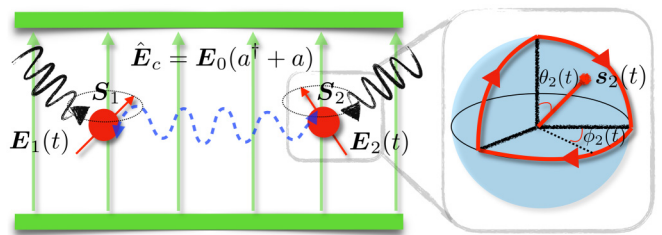


FIG. 1. Left: Sketch of the two-hole-spin $S = 3/2$ system coupled to a cavity field $\hat{E}_c = E_0(a^\dagger + a)$. Each of the two spins $j = 1, 2$ is driven by a classical time-periodic electrical field $E_j(t + T_j) = E_j(t)$, with T_j the corresponding period. The cavity induces a time-dependent coupling between the two spins (blue wavy line). Right: The evolution of one of the effective qubits in the degenerate low-energy sector on the Bloch sphere during the adiabatic driving. Here, $s_2(t)$ is the instantaneous direction of the effective magnetic field quantified by the angles $\theta_2(t)$ and $\phi_2(t)$, while in red we exemplify one possible cyclic trajectory.

^{*}wysockinski@magtop.ifpan.edu.pl

[†]mtrif@magtop.ifpan.edu.pl

spins 3/2 coupled to the electric field of a microwave cavity. The minimal Hamiltonian describing the system reads [17]

$$H_{\text{tot}}(t) = \sum_{j=1,2} d_j [E_{j,\alpha}(t) + E_{0,\alpha}(a^\dagger + a)] \Gamma_j^\alpha + \omega_0 a^\dagger a, \quad (1)$$

where d_j is the spin-electric field coupling strength of spin $j = 1, 2$, $E_{j,\alpha}(t)$ and $E_{0,\alpha}$ are the $\alpha = x, y, z$ components of the $j = 1, 2$ (time-dependent) external and cavity electric field, respectively, while a (a^\dagger) is the photon annihilation (creation) operator, with ω_0 being the bare cavity frequency. Also, the matrices Γ_j^n , with $n \in \{1, 5\}$, are the generators of the SO(5) Clifford algebra for spin j [17,34]. The above Hamiltonian is precisely that of Ref. [17] proposed to process spin-3/2 valence band impurities in III-V semiconductors, but accounting for a quantum electrical field stemming from the cavity on top of the time-dependent classical drive. There, the coupling to the electrical field originates from the linear Stark effect allowed by the diamond T_d symmetry, as it is the case of acceptor spins in Si [35]. In such cases, $d = ea_B \chi$, with e , a_B , and χ being the electron charge, the Bohr radius, and the dimensionless dipolar parameter, respectively [36,37]. More complicated terms, such as the quadrupolar couplings [20], can be accounted for within the same framework by extending the couplings to all the Γ_j^n matrices. For simplicity, in the following we substitute $d_j E_{0,\alpha} \equiv g_{j,\alpha}$ and take $d_j = 1$. In the presence of an electric field the time-reversal symmetry is preserved and each spin 3/2 is described by two doubly degenerate instantaneous states.

Adiabatic perturbation theory. For static external fields, and in the absence of the cavity, the spectrum consists of (at least) double degenerate levels, a consequence of the Kramers theorem. In the adiabatic limit, quantified by $\dot{E}_{j,\alpha}/E_{j,\alpha} \ll 2\epsilon_j$, with $2\epsilon_j = 2\sqrt{\sum_\alpha E_{j,\alpha}^2(t)}$ being the instantaneous spin splitting of hole j , as well as for weak spin-photon coupling $|g_j| \ll |\epsilon_j - \omega_0|$, we can treat both the dynamics and the coupling to photons in time-dependent perturbation theory. In the following, we extend the approach in Ref. [38] used to single out the geometrical effects in degenerate systems to the $S = 3/2$ spin system. In contrast to Ref. [38], however, we treat the environment (cavity photons) on the same footing with the two spins 3/2. The full technical details are left for the Supplemental Material (SM) [34], while here we only describe the steps and summarize the results. That entails first performing a time-dependent unitary transformation, $U(t) = U_1(t)U_2(t)$, that diagonalizes each of the isolated spin-3/2 Hamiltonians, so that $\tilde{H}_{\text{tot}}(t) = \omega_0 n_{\text{ph}} + \sum_j [H_{j,0}(t) + V_j(t)]$, where $H_{j,0}(t) = \epsilon_j(t) \Gamma_j^5$ is the unperturbed part of the spin $j = 1, 2$ Hamiltonian [38], with $n_{\text{ph}} \equiv a^\dagger a$, and

$$V_j(t) = \dot{E}_{j,\alpha} \mathcal{A}_{j,\alpha} + g_{j,\alpha} (\partial_\alpha \epsilon_j \Gamma_j^5 + i\epsilon_j [\mathcal{A}_{j,\alpha}, \Gamma_j^5]) X_{\text{ph}}. \quad (2)$$

Here, $\mathcal{A}_{j,\alpha} = -iU_j^\dagger(t) \partial_{E_{j,\alpha}} U_j(t)$ is the non-Abelian gauge field pertaining to the electric field $E_{j,\alpha}$ with $\partial_\alpha \equiv \partial_{E_{j,\alpha}}$, and $X_{\text{ph}} = (a^\dagger + a)$. Note that $V_j(t)$ leads to both diagonal and off-diagonal transitions between the degenerate eigenstates of the bare spin Hamiltonian $H_{j,0}(t)$. Next, we can treat the $\dot{E}_{j,\alpha}$ and $V_j(t)$ in perturbation theory with respect to the spin splittings ϵ_j and photon frequency ω_0 using a time-dependent Schrieffer-Wolff (SW) transformation $U'(t) = U'_1(t)U'_2(t)$,

with $U'_j(t) = e^{-S_j(t)} \approx 1 - S_j(t) + S_j^2(t)/2 + \dots$. By imposing $[S_j(t), H_{j,0} + \omega_0 a^\dagger a] + V_j(t) = 0$, it allows us to keep the leading diagonal terms in the velocities $\dot{E}_{j,\alpha}$ and the second-order corrections in $g_{j,\alpha}$. Then, projecting onto the low four-dimensional energy subspace spanned by the $\{-\epsilon_1, -\epsilon_2\}$, we can find an explicit expression for $S_j(t)$ (see SM for details). That in turn allows us to obtain the low-energy spin-photon Hamiltonian $\delta\mathcal{H}(t) = \sum_j \delta\mathcal{H}_j(t) + \mathcal{H}_{1-2}(t)$, with

$$\begin{aligned} \delta\mathcal{H}_j(t) &= \dot{E}_{j,\alpha} g_{j,\beta} (\mathcal{F}_{j,\alpha\beta}^l X_{\text{ph}} + g_{j,\gamma} \mathcal{O}_{j,\alpha\beta\gamma}^l n_{\text{ph}}), \\ \mathcal{H}_{1-2}(t) &= \frac{2g_{1,\alpha} g_{2,\beta}}{\omega_0} \dot{E}_{1,\gamma} \dot{E}_{2,\delta} \mathcal{F}_{1,\alpha\gamma}^l \mathcal{F}_{2,\beta\delta}^l, \end{aligned} \quad (3)$$

representing the photon-dependent single hole-spin Hamiltonian and the cavity-mediated spin-spin coupling term, respectively. Here, $\mathcal{A}_{j,\alpha}^l \equiv \mathcal{P}_j^l \mathcal{A}_{j,\alpha} \mathcal{P}_j^l$, with \mathcal{P}_j^l a projector onto the low-energy degenerate subspace of spin j , $\mathcal{F}_{j,\alpha\beta}^l = \partial_\alpha \mathcal{A}_{j,\beta}^l - \partial_\beta \mathcal{A}_{j,\alpha}^l + i[\mathcal{A}_{j,\alpha}^l, \mathcal{A}_{j,\beta}^l]$ is the corresponding non-Abelian Berry curvature, and $\mathcal{O}_{j,\alpha\beta\gamma}^l$ is an operator that encodes also the geometry of the states. In particular, for $\omega_0 \ll \epsilon_{1,2}$, this can be written as

$$\begin{aligned} \mathcal{O}_{j,\alpha\beta\gamma}^l &= i[\partial_\alpha \mathcal{A}_{j,\beta}^l, \mathcal{A}_{j,\gamma}^l] - 2\partial_\beta \log[\epsilon_j] \mathcal{F}_{j,\gamma\alpha}^l \\ &\quad - 2(\mathcal{G}_{j,\beta\gamma}^l \mathcal{A}_{j,\alpha}^l - \mathcal{A}_{j,\beta}^- \mathcal{A}_{j,\alpha}^h \mathcal{A}_{j,\gamma}^+), \end{aligned} \quad (4)$$

where $[\dots]^l \equiv \mathcal{P}_j^l [\dots] \mathcal{P}_j^l$, $\mathcal{G}_{j,\beta\gamma}^l$ is the quantum metric in the lowest subspace [34], and $\mathcal{A}_{j,\alpha}^h \equiv \mathcal{P}_j^h \mathcal{A}_{j,\alpha} \mathcal{P}_j^h$, with $\mathcal{P}_j^h = 1 - \mathcal{P}_j^l$ being the Berry curvature in the highest-energy subspace of spin, and $\mathcal{A}_{j,\alpha}^{+(-)} \equiv \mathcal{P}_j^{h(l)} \mathcal{A}_{j,\alpha} \mathcal{P}_j^{(h)}$. The Hamiltonians in Eq. (3) are the central results of this Letter, showing that photons in a cavity can be imprinted with the individual hole-spin Berry phases and, moreover, they can mediate interactions between two hole spins via the geometry of their states in the absence of any external magnetic fields. Therefore, such effects are present only if the spins are driven, providing the means for selectively entangling spin-3/2 qubits coupled to the same cavity field. Notably, the above Hamiltonians depend only on the geometry of states through their Berry connections, being thus general and applicable, we believe, to any non-Abelian system. Although the Hamiltonian $\mathcal{H}_{1-2}(t) \propto \dot{E}_{1,\gamma} \dot{E}_{2,\delta}$, the evolution operator endowed by this term is effectively geometrical when the two driving frequencies $\Omega_{1,2}$ (in a continuous operation mode) are incommensurate [34,39], as we show explicitly later.

The first term in $\delta\mathcal{H}_j(t)$ in Eq. (3) describes the leading order coupling of the degenerate spin-3/2 subspace to the photons, in agreement with the findings in Ref. [38]. This term can be leveraged in order to manipulate the qubit by driving the cavity with a classical (coherent) field. The second contribution instead is different and accounts for the cavity frequency shift induced by the individual hole-spin geometry of states. Thus, we have extended the dispersive readout of geometrical Abelian Berry phases [40,41] to the non-Abelian realm. While seemingly complicated, the origin of each term in $\mathcal{O}_{j,\alpha\beta\gamma}^l$ can be unraveled by using a Floquet approach for describing the dynamics [34]. Interestingly, for $\omega_0 \sim \dot{E}_{j,\alpha}/\epsilon_j$, the photons and the external driving become resonant, and given that generally $[\mathcal{A}_{j,\alpha}^l, \mathcal{F}_{j,\alpha\beta}^l] \neq 0$, it can result in a

different type of Jaynes-Cummings Hamiltonian that is activated by the geometry of the states. Nevertheless, we leave this aspect for future work, and focus here on the regime $\omega_0 \gg \dot{E}_{j,\alpha}/\epsilon_j$.

Dispersive Floquet approach. Next we utilize a Floquet description of the hole-spin dynamics that is appropriate when each of the spins 3/2 is driven periodically, or $H_j(t) = H_j(t) [H_j(t) \equiv E_{j,\alpha}(t)\Gamma_j^\alpha]$, with $\Omega_j = 2\pi/T_j$ being the driving frequency of spin $j = 1, 2$. In the absence of the cavity, the time-dependent wave functions (or Floquet states) can be written as $|\Psi_j^s(t)\rangle = e^{-i\mathcal{E}_j^s t} |\psi_j^s(t)\rangle$, where $|\psi_j^s(t+T_j)\rangle = |\psi_j^s(t)\rangle$ is found as solutions to the Schrödinger equation $\mathcal{H}_j(t)|\psi_j^s(t)\rangle \equiv [H_j(t) - i\partial/\partial t]|\psi_j^s(t)\rangle = \mathcal{E}_j^s |\psi_j^s(t)\rangle$, and \mathcal{E}_j^s are the Floquet eigenvalues for spin j that are defined up to multiple of Ω_j , with $s = 1, 2, \dots$ labeling the periodic Floquet states. In the adiabatic limit, $\mathcal{E}_j^s = \epsilon_j^s + \gamma_j^s/T_j$, with ϵ_j^s and γ_j^s being the instantaneous (or average) energy and the Berry phase of the spin j in the Floquet state s . Coupling the spins to the photons results in both shifts in the individual Floquet energies and a coupling between the two spins. The full dynamics of the two spins driven at different frequencies is rather involved (see, for example, Ref. [39]), and here instead we focus on the weak coupling regime in the dispersive limit, that is, when $|\Delta_j^{ss'}(q) - \omega_0| \gg |\mathbf{g}_{1,2}|$, with $\Delta_j^{ss'}(q) = |\mathcal{E}_j^s - \mathcal{E}_j^{s'} - q\Omega_j|$ and $q \in \mathcal{Z}$, which allows us to treat the spin-photon interaction in perturbation theory. Using a time-dependent SW transformation, which is described in detail in the SM, the cavity induced low- (quasi-)energy spin Hamiltonian can be cast as $\delta\mathcal{H} = \sum_j \delta\mathcal{H}_j + \mathcal{H}_{1-2}^z + \mathcal{H}_{1-2}^\perp$, with

$$\begin{aligned} \delta\mathcal{H}_j &= n_{\text{ph}} \sum_{q,s,s'} (-1)^s |V_j^{ss'}(q)|^2 \frac{\Delta_j^{ss'}(q)}{[\Delta_j^{ss'}(q)]^2 - \omega_0^2} \sigma_j^z, \\ \mathcal{H}_{1-2}^z &= \frac{2}{\omega_0} \sum_{j,s,p \in \text{low}} (-1)^{s+p} V_j^{ss}(0) V_j^{pp}(0) \sigma_1^z \sigma_2^z, \\ \mathcal{H}_{1-2}^\perp &= \sum_j V_j^{12}(0) V_j^{21}(0) \frac{2\omega_0}{\omega_0^2 - [\Delta_j^{12}(0)]^2} \sigma_1^+ \sigma_2^- + \text{H.c.}, \end{aligned} \quad (5)$$

where $V_j^{ss'}(q) = (1/T_j) \int_0^{T_j} dt e^{-iq\Omega_j t} \langle \psi_j^s(t) | \mathbf{g}_j \cdot \boldsymbol{\Gamma}_j | \psi_j^{s'}(t) \rangle$ are the Fourier components of the spin-photon matrix elements between states s and s' and spin $j = 1, 2$. Also, σ_j^α , with $\alpha = x, y, z$, are Pauli matrices acting in the two lowest- (quasi-)energy Floquet states of the hole spin $j = 1, 2$. The first term leads to a cavity frequency shift that depends on the Floquet state of spin j , while the second and third terms account for an Ising and XY couplings between the lowest spin Floquet doublets, respectively. As showed in detail in the SM, in the adiabatic limit $\Omega_j \ll |E_j|$ we find that $\delta\mathcal{H}_j \propto \Omega_j$ and $\mathcal{H}_{1-2}^\perp \propto \Omega_1 \Omega_2$, consistent with the expressions found in the previous section. Note that \mathcal{H}_{1-2}^\perp depend only on the $q = 0$ Fourier components of $V_j^{ss'}(t)$ which, as argued before, result in geometrical effects only on the evolution. All these effects are absent in the static case and, in particular, the entanglement between the Floquet states is ignited only by driving *both* spins.

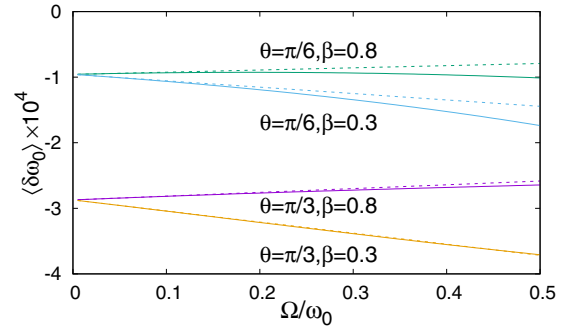


FIG. 2. Cavity frequency shift $\langle \delta\omega_0 \rangle$ due to the interaction with a single hole spin as a function of driving frequency Ω for several cone angles θ and initial superposition weights β . The solid (dashed) lines represent the result without (with) an adiabatic approximation. The other parameters are $\omega_0 = 0.15$, $\epsilon = 1.05$, $g = 0.02$, and the spin-photon coupling is set along the z axis.

Circular driving. In order to verify both the adiabatic theory and the above Floquet approach, in this section we consider a specific model, namely that of a circularly driven spin 3/2. Without loss of generality in the following we shall use parametrization, $\mathbf{E}_j = \epsilon_j \mathbf{n}_j(t)$ and $\mathbf{n}_j(t) = \{-\sin \theta_j \sin \Omega_j t, \sin \theta_j \cos \Omega_j t, \cos \theta_j\}$, where Ω_j and θ_j are again the driving frequency and the cone angle for the j th spin. We were able to find a time-dependent transformation $\tilde{U}(t)$ (for details, see SM) that makes the bare hole-spin part of $H_{\text{tot}}(t)$ fully time-independent and diagonal, i.e., it gives access to the exact solution in the absence of the cavity. Therefore, the entire time dependence of the spin-photon system in this frame is shifted to the spin-photon interactions. Then, in the dispersive regime we can decouple the spin and photonic degrees of freedom by means of the second-order SW transformation in \mathbf{g}_j , and the resulting low-energy spin-photon Hamiltonian assumes the same form as in Eq. (5) with $\mathcal{H}_{1-2}^\perp = 0$. In general, $\delta\mathcal{H}_j = \delta\omega_{0,j}^s(t) \sigma_j^z n_{\text{ph}}$ and $\mathcal{H}_{1-2}^z(t) = J_{1-2}^z(t) \sigma_1^z \sigma_2^z$, with $J_{1-2}^z(t) = -(\Omega_1 \Omega_2 / 2\omega_0) f_1(t) f_2(t)$ and $f_j(t+T_j) = f_j(t)$ [cf. Eq. (41) in SM [34]]. For $\mathbf{g}_j = \{0, 0, g_j\}$ and in leading order in Ω_j , we obtain [34]

$$\delta\omega_{j,0}^s = - \frac{2g_j^2 \Omega_j (12\epsilon_j^2 - \omega_0^2) \cos \theta_j \sin^2 \theta_j}{(4\epsilon_j^2 - \omega_0^2)^2}, \quad (6)$$

$$f_j = \frac{g_j \sin^2 \theta_j}{\epsilon_j}, \quad (7)$$

while $\mathcal{H}_j = (1/2)\Omega_j \cos \theta_j \sigma_j^z$ (bare low-energy hole-spin Hamiltonian). Above, $\delta\omega_{j,0}^s$ is the cavity frequency shift pertaining to the geometrical imprints of the lowest-energy sector, while we disregarded the (dynamical) contributions $\delta\omega_{j,0}^d$ that can shift the cavity frequency by a value independent of the qubit state [34].

In the following, we demonstrate numerically that in the presence of the driving the cavity frequency shift provides a readout of the non-Abelian evolution. Given an initial hole-spin state at time $t = 0$, $|\psi(0)\rangle = \{\sqrt{1-\beta^2}, \beta e^{i\phi}\}$, we can evaluate the geometrical contribution during the periodic evolution as $\langle \delta\omega_0^s \rangle = (1/T) \int_0^T \langle \psi(t) | \sigma^z | \psi(t) \rangle \delta\omega_0^s$, where $|\psi(t)\rangle \equiv \mathcal{U}(t) |\psi(0)\rangle$ with the evolution operator $\mathcal{U}(t)$

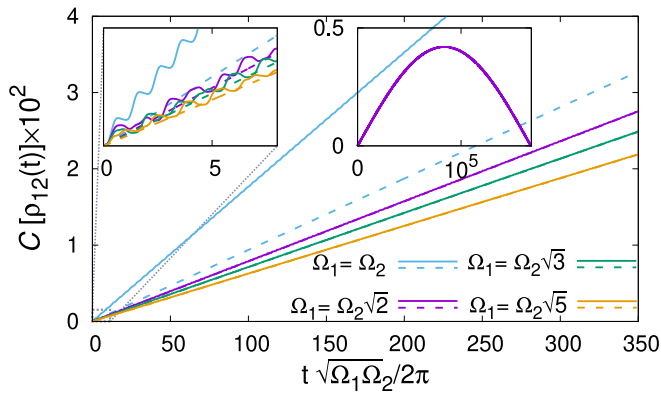


FIG. 3. The concurrence $C[\rho_{12}(t)]$ pertaining to the two-qubit density matrix $\rho_{12}(t)$ as a function of time for various driving Ω_1/Ω_2 ratios. With dashed lines we mark the concurrence generated by the effective static $\mathcal{H}_{1-2}^{z,g}$. The left inset depicts the short time behavior of the concurrence exhibiting fast oscillations, while the right inset shows a nonmonotonic behavior of the concurrence for long times $t \simeq \hbar/J_{1-2}^z$ for $\sqrt{2}\Omega_2 = \Omega_1$. We have used following parametrization: $\omega_0 = 0.15$, $g = 0.02$, $\epsilon_1 = 1.05$, $\epsilon_2 = 0.95$, $\Omega_1 = 0.1$, $\mathbf{g}_1 = g\{1/2, 1/2, 1/\sqrt{2}\}$, $\mathbf{g}_2 = g\{1/\sqrt{2}, 1/2, 1/2\}$, $\theta_1 = \pi/3$, $\theta_2 = \pi/4$, $\beta_1 = 0.4$, and $\beta_2 = 0.3$.

describing the bare hole-spin Hamiltonian. In linear order Ω , we find the simple functional dependence $\langle \delta\omega_0^g \rangle = (2\beta^2 - 1)\delta\omega_0^g$, which allows us to discriminate between different qubit states. As expected, in the absence of the driving, $\langle \delta\omega_0^g \rangle = 0$. In Fig. 2 we plot the total photonic frequency shift $\langle \delta\omega_0 \rangle \equiv \langle \delta\omega_0^d \rangle + \langle \delta\omega_0^g \rangle$ obtained from evolving the full spin $S = 3/2$ Hamiltonian and that obtained from the adiabatic, low-energy approximation, respectively as a function of the driving frequency Ω for various values of β [34]. We see that the adiabatic approximation (linear in Ω) describes well the frequency shift for a wide range of parameters [34].

Finally, we demonstrate the entangling properties of the Hamiltonian $\mathcal{H}_{1-2}^z(t)$. Before that, it is instructive to define an effective static Hamiltonian, $\mathcal{H}_{1-2}^{z,g} = J_{1-2}^{z,g} \sigma_1^z \sigma_2^z$ with $J_{1-2}^{z,g} = -\Omega_1 \Omega_2 f_1^0 f_2^0 / 2\omega_0$, where $f_j^0 = (\Omega_j / 2\pi) \int_0^{2\pi/\Omega_j} d\tau f_j(\tau)$ is the $q = 0$ Fourier component of $f_j(t)$. Since each closed spin trajectory is contributing individually here, $\mathcal{H}_{1-2}^{z,g}$ is inherently geometrical (external noises affect its evolution similarly to geometrical gates). For a given two-qubit density matrix $\rho_{12}(t)$, the entanglement can be quantified by the concurrence $C[\rho_{12}(t)] = \max[0, \lambda_{12}^1 - \lambda_{12}^2 - \lambda_{12}^3 - \lambda_{12}^4]$ [42], where the λ_{12}^k are the eigenvalues of the Hermitian matrix $R_{12} = \sqrt{\rho_{12}} \tilde{\rho}_{12} \sqrt{\rho_{12}}$ sorted in descending order with $\tilde{\rho}_{12} = (\sigma_1^y \otimes \sigma_2^y) \rho_{12}^* (\sigma_1^y \otimes \sigma_2^y)$. The concurrence is $C = 0(1)$ for a separable (maximally entangled) state. Starting from a separable density matrix at $t = 0$, in Fig. 3 we show $C[\rho_{12}(t)]$ as a

function of time when the evolution is generated by the full time-dependent $\mathcal{H}_{1-2}^z(t)$ Hamiltonian and by the effective static Hamiltonian $\mathcal{H}_{1-2}^{z,g}$. We see excellent (poor) agreement between the two cases when the driving frequencies are incommensurate (commensurate), demonstrating the geometrical origin of the entanglement at incommensurate drives. Note that $C[\rho_{12}(t)]$ increases with time, becoming maximal for $t \sim \hbar/J_{1-2}^z$ (cf. the right inset of Fig. 3). Furthermore, we also analyzed the robustness of the entanglement generation to noises in the driving frequencies, $\Omega_j t \rightarrow \phi_j(t) \equiv \Omega_j t + \delta_j(t)$, with $\delta_j(t)$ being a Gaussian correlated noise [39]. We have evaluated $\kappa = |C_0(t) - \overline{C}(t)|$, where $C_0(t)$ is a noiseless concurrence and $\overline{C}(t)$ is the mean concurrence, and we found that κ is almost two orders of magnitude smaller in the case of incommensurate drives as compared to the commensurate ones [34]. That is again consistent with the enhanced protection associated with geometrical qubits [33].

In order to give some estimates for the strength of the exchange coupling induced by the dynamics presented in this Letter, we utilize the GaAs quantum dot model proposed in Ref. [20]. We assume for the hole-spin splittings $\epsilon_1 = \epsilon_2 = 0.285$ meV (which corresponds to electrical fields in the range of 10^5 – 10^6 V/m), $\omega_0 \simeq 10$ GHz, driving frequency $\Omega_1 = \sqrt{2}\Omega_2 = 0.043$ THz, and spin-cavity coupling strengths $g_1 = g_2 = 5.7$ μ eV. For a cavity field parallel to the z axis, the spin-spin interaction is maximized for $\theta_1 = \theta_2 = \pi/2$, as showed in Eq. (7), and we obtain $J_{1-2}^z \simeq 2.7$ neV, or a two-qubit gate time of 10^{-5} s. This timescale is much shorter than the coherence times of a single spin-hole qubit that can be as high as 10 ms [43].

Conclusions. We have proposed and studied an all-electrical scheme for entangling hole spins in nanostructures using the non-Abelian character of their states and the electrical field of a microwave cavity. We showed that the Berry phases of electrically driven hole spins imprint onto the cavity photons allowing for a dispersive readout of the hole-spin qubit. Furthermore, we have shown that the cavity mediates long-range entangling coupling between the non-Abelian Berry curvatures of two hole spins when both are electrically driven, enabling selective entanglement between hole-spin qubits. Our work might be relevant for a plethora of other solid-state qubits with a nontrivial geometry of states, such as electrons localized in quantum dots or molecular magnets.

Acknowledgments. This work was supported by the International Centre for Interfacing Magnetism and Superconductivity with Topological Matter project, carried out within the International Research Agendas program of the Foundation for Polish Science cofinanced by the European Union under the European Regional Development Fund. We would like to thank S. Hoffman and A. Lau for useful discussions.

- [1] D. Loss and D. P. DiVincenzo, *Phys. Rev. A* **57**, 120 (1998).
 [2] B. E. Kane, *Nature (London)* **393**, 133 (1998).
 [3] J. R. Petta, A. C. Johnson, J. M. Taylor, E. A. Laird, A. Yacoby, M. D. Lukin, C. M. Marcus, M. P. Hanson, and A. C. Gossard, *Science* **309**, 2180 (2005).

- [4] J. J. L. Morton, A. M. Tyryshkin, R. M. Brown, S. Shankar, B. W. Lovett, A. Ardavan, T. Schenkel, E. E. Haller, J. W. Ager, and S. A. Lyon, *Nature (London)* **455**, 1085 (2008).
 [5] D. D. Awschalom, L. C. Bassett, A. S. Dzurak, E. L. Hu, and J. R. Petta, *Science* **339**, 1174 (2013).

- [6] M. Veldhorst, C. H. Yang, J. C. C. Hwang, W. Huang, J. P. Dehollain, J. T. Muhonen, S. Simmons, A. Laucht, F. E. Hudson, K. M. Itoh *et al.*, *Nature (London)* **526**, 410 (2015).
- [7] F. H. L. Koppens, C. Buizert, K. J. Tielrooij, I. T. Vink, K. C. Nowack, T. Meunier, L. P. Kouwenhoven, and L. M. K. Vandersypen, *Nature (London)* **442**, 766 (2006).
- [8] S. Nadj-Perge, S. M. Frolov, E. P. A. M. Bakkers, and L. P. Kouwenhoven, *Nature (London)* **468**, 1084 (2010).
- [9] Y. Hu, F. Kuemmeth, C. M. Lieber, and C. M. Marcus, *Nat. Nanotechnol.* **7**, 47 (2012).
- [10] J. T. Muhonen, J. P. Dehollain, A. Laucht, F. E. Hudson, R. Kalra, T. Sekiguchi, K. M. Itoh, D. N. Jamieson, J. C. McCallum, A. S. Dzurak *et al.*, *Nat. Nanotechnol.* **9**, 986 (2014).
- [11] S. D. Liles, R. Li, C. H. Yang, F. E. Hudson, M. Veldhorst, A. S. Dzurak, and A. R. Hamilton, *Nat. Commun.* **9**, 3255 (2018).
- [12] V. N. Golovach, A. Khaetskii, and D. Loss, *Phys. Rev. Lett.* **93**, 016601 (2004).
- [13] Y. A. Serebrennikov, *Phys. Rev. Lett.* **93**, 266601 (2004).
- [14] P. San-Jose, G. Zarand, A. Shnirman, and G. Schön, *Phys. Rev. Lett.* **97**, 076803 (2006).
- [15] B. D. Gerardot, D. Brunner, P. A. Dalgarno, P. Öhberg, S. Seidl, M. Kroner, K. Karrai, N. G. Stoltz, P. M. Petroff, and R. J. Warburton, *Nature (London)* **451**, 441 (2008).
- [16] M. Trif, P. Simon, and D. Loss, *Phys. Rev. Lett.* **103**, 106601 (2009).
- [17] B. A. Bernevig and S.-C. Zhang, *Phys. Rev. B* **71**, 035303 (2005).
- [18] P. San-Jose, B. Scharfenberger, G. Schön, A. Shnirman, and G. Zarand, *Phys. Rev. B* **77**, 045305 (2008).
- [19] V. N. Golovach, M. Borhani, and D. Loss, *Phys. Rev. A* **81**, 022315 (2010).
- [20] J. C. Budich, D. G. Rothe, E. M. Hankiewicz, and B. Trauzettel, *Phys. Rev. B* **85**, 205425 (2012).
- [21] J. Fischer, W. A. Coish, D. V. Bulaev, and D. Loss, *Phys. Rev. B* **78**, 155329 (2008).
- [22] D. V. Bulaev and D. Loss, *Phys. Rev. Lett.* **95**, 076805 (2005).
- [23] D. Heiss, S. Schaeck, H. Huebl, M. Bichler, G. Abstreiter, J. J. Finley, D. V. Bulaev, and D. Loss, *Phys. Rev. B* **76**, 241306(R) (2007).
- [24] D. Brunner, B. D. Gerardot, P. A. Dalgarno, G. Wüst, K. Karrai, N. G. Stoltz, P. M. Petroff, and R. J. Warburton, *Science* **325**, 70 (2009).
- [25] R. J. Warburton, *Nat. Mater.* **12**, 483 (2013).
- [26] A. P. Higginbotham, T. W. Larsen, J. Yao, H. Yan, C. M. Lieber, C. M. Marcus, and F. Kuemmeth, *Nano Lett.* **14**, 3582 (2014).
- [27] J. van der Heijden, J. Salfi, J. A. Mol, J. Verduijn, G. C. Tettamanzi, A. R. Hamilton, N. Collaert, and S. Rogge, *Nano Lett.* **14**, 1492 (2014).
- [28] H. Watzinger, J. Kukucka, L. Vukusić, F. Gao, T. Wang, F. Schäffler, J.-J. Zhang, and G. Katsaros, *Nat. Commun.* **9**, 3902 (2018).
- [29] S. Asaad, V. Mourik, B. Joecker, M. A. I. Johnson, A. D. Baczewski, H. R. Firgau, M. T. Mądzik, V. Schmitt, J. J. Pla, F. E. Hudson *et al.*, *Nature (London)* **579**, 205 (2020).
- [30] N. W. Hendrickx, D. P. Franke, A. Sammak, G. Scappucci, and M. Veldhorst, *Nature (London)* **577**, 487 (2020).
- [31] J. E. Avron, L. Sadun, J. Segert, and B. Simon, *Phys. Rev. Lett.* **61**, 1329 (1988).
- [32] J. E. Avron, L. Sadun, J. Segert, and B. Simon, *Commun. Math. Phys.* **124**, 595 (1989).
- [33] P. Zanardi and M. Rasetti, *Phys. Lett. A* **264**, 94 (1999).
- [34] See Supplemental Material at <http://link.aps.org/supplemental/10.1103/PhysRevB.104.L041402> for details of the calculations.
- [35] J. Salfi, J. A. Mol, D. Culcer, and S. Rogge, *Phys. Rev. Lett.* **116**, 246801 (2016).
- [36] G. Bir, E. Butikov, and G. Pikus, *J. Phys. Chem. Solids* **24**, 1475 (1963).
- [37] P. Philippopoulos, S. Chesi, D. Culcer, and W. A. Coish, *Phys. Rev. B* **102**, 075310 (2020).
- [38] K. Snizhko, R. Egger, and Y. Gefen, *Phys. Rev. B* **100**, 085303 (2019).
- [39] I. Martin, G. Refael, and B. Halperin, *Phys. Rev. X* **7**, 041008 (2017).
- [40] S. Kohler, *Phys. Rev. Lett.* **119**, 196802 (2017).
- [41] M. Trif and P. Simon, *Phys. Rev. Lett.* **122**, 236803 (2019).
- [42] W. K. Wootters, *Phys. Rev. Lett.* **80**, 2245 (1998).
- [43] T. Kobayashi, J. Salfi, C. Chua, J. van der Heijden, M. G. House, D. Culcer, W. D. Hutchison, B. C. Johnson, J. C. McCallum, H. Riemann *et al.*, *Nat. Mater.* **20**, 38 (2021).